

Electronic Supplementary Information (ESI)

1) Supplementary calculation methods during the evaluation of electrochemical performances

A: The calculation method of specific capacitance in single-electrode tests

Firstly, the charge (Q , C) obtained from CV curves was calculated by

$$Q = \frac{1}{2\nu} \oint I(V) dV \quad (1)$$

Where ν is the scan rate with unit of Volt per second (V/s), $I(V)$ is the current response as the function of applied Voltage (V) with unit of Ampere (A).

Using equation (1), the charges of 3D graphene/carbon nanotubes/MnO₂ (3DG/CNTs/MnO₂) (Q_1) and 3DG/CNTs (Q_2) were calculated, respectively.

Secondly, the specific capacitance (C_s , F/g) of MnO₂ was calculated from

$$C_s = \frac{Q_1 - Q_2}{m \cdot \Delta V} \quad (2)$$

Where Q_1 and Q_2 are the charges of 3DG/CNTs/MnO₂ and 3DG/CNTs respectively, m is the mass loading of active materials in the composite electrode with unit of gram (g), ΔV is potential window for the charge/discharge process with unit of Volt (V).

Similarly, the specific capacitance of MnO₂ in 3DG/MnO₂ was also calculated similarly from the above mentioned equations. Additionally, the specific capacitance of activated carbon (AC) in 3DG/AC was also calculated from the above mentioned equations to assemble optimized asymmetric supercapacitor.

B. The optimizing method to balance the charges on positive and negative electrodes in the asymmetric supercapacitor

The charges stored by each electrode depends on the specific capacitance (C_s), the potential window for the charge/discharge process (ΔV) and the mass of the active materials in electrode (m) following the Equation¹

$$Q = C_s \times \Delta V \times m \quad (3)$$

So, the balance between the charges on positive and negative electrodes can be represented by

$$C_s^+ \times \Delta V^+ \times m^+ = C_s^- \times \Delta V^- \times m^- \quad (4)$$

That is

$$\frac{m^-}{m^+} = \frac{C_s^+ \times \Delta V^+}{C_s^- \times \Delta V^-} \quad (5)$$

In our study, the C_s were obtained from the CVs (shown in Figure S6) of single electrode at 10 mV/s, and they are 239.3 F/g and 217.6 F/g for the positive and negative electrodes, respectively. The potential ranges of positive and negative electrodes were from 0 to 1 V and from -1 to 0 V, respectively, so the ΔV is equivalent as 1 V for the two electrodes. Finally, 0.92 mg AC was matched in 3DG/AC, according to the equation (5) with the known mass of MnO₂ (0.84 mg) in positive electrode.

C. The calculation method of power density and energy density in assembled supercapacitor tests

The average specific capacitance (C , F/g), the energy density (E , Wh/kg), and the power density (P , W/kg) were calculated from GCDs at different charge/discharge currents by the following equations

$$C = \frac{I \cdot \Delta t}{M \cdot \Delta V} \quad (6)$$

$$E = \frac{1}{2} \cdot C \cdot V^2 \quad (7)$$

$$P = \frac{E}{\tau} = \frac{1}{2M} \cdot I \cdot V \quad (8)$$

Where I is charge/discharge current, Δt is discharge time, ΔV is discharge potential, M is the total active materials' mass of two electrodes, and V is the sweep potential window.

2) Supplementary figures and table

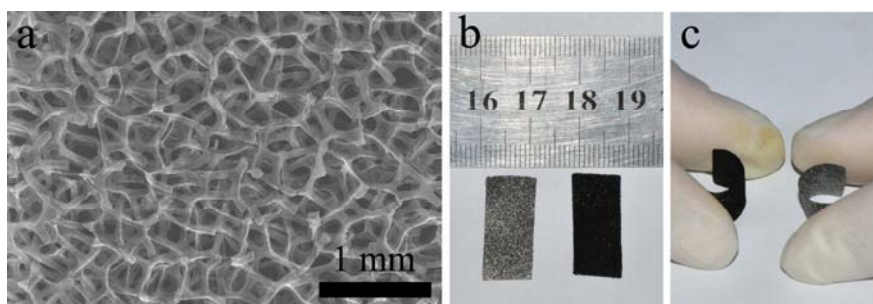


Fig. S1. SEM image (a) demonstrates that the as prepared 3DG copies the porous structure completely after removing Ni foam. From the optical photos of 3DG and 3DG/CNTs shown in (b) and (c), it is found that the color of 3DG turned from gray to dark after the growth of CNTs, and they are keeping the free-standing form, and possess flexible property.

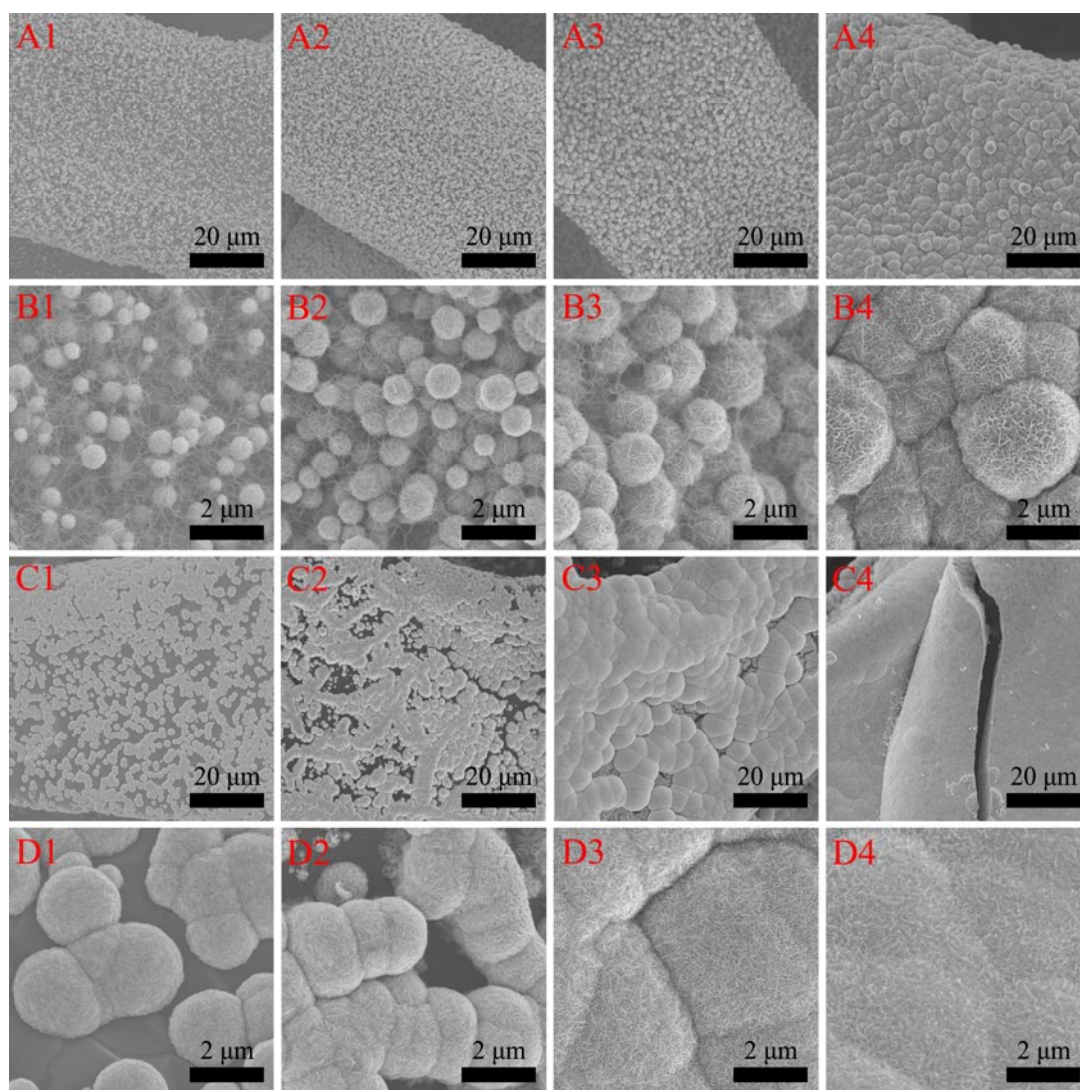


Fig. S2. SEM images of 3DG/CNTs/MnO₂ and 3DG/MnO₂. A1 (B1), A2 (B2), A3 (B3) and A4 (B4) are low (high) magnitude images of 3DG/CNTs/MnO₂ with 0.5 h, 2 h, 6 h and 12 h MnO₂ deposition, respectively. C1 (D1), C2 (D2), C3 (D3) and C4 (D4) are low (high) magnitude images of 3DG/MnO₂ with 0.5 h, 2 h, 6 h and 12 h MnO₂ deposition, respectively.

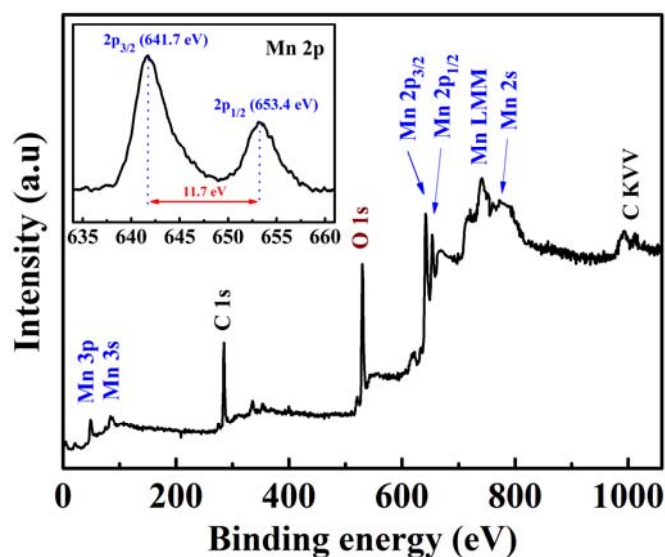


Fig. S3. XPS spectrum of the 3DG/CNTs/MnO₂, the inset is the Mn 2p core level spectrum.

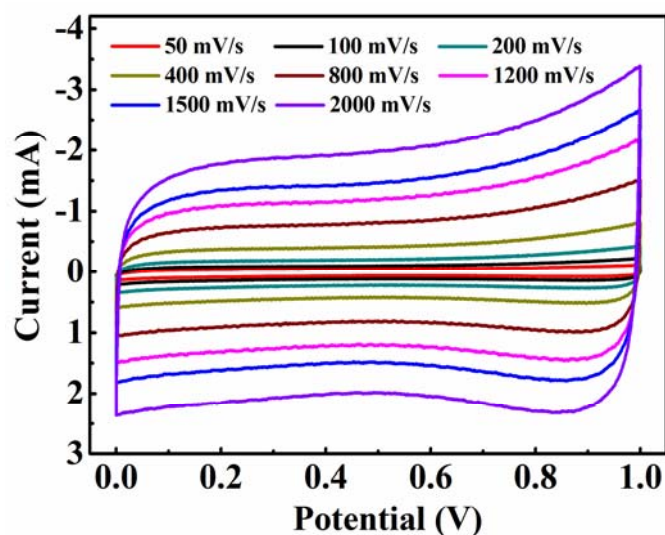


Fig. S4. CVs of 3DG/CNTs at various scan rates in 1 M Na₂SO₄ aqueous solution.

The CVs exhibit almost symmetrical rectangular shape even at the highest scan rates of 2000 mV/s, indicating its ideal double layer capacitive property and stable rate capability. These results demonstrate that the 3DG/CNTs are better choice of electrodes and collectors for supercapacitors to suffer high scan rate even up to 2000 mV/s. Yet from the current responses of CVs, it is deduced that the capacitance contribution from the 3DG/CNTs is insignificant, because the current responses are 1-3 orders lower than those of 3DG/CNTs/MnO₂-0.5. Therefore, only the specific capacitance of MnO₂ is taken into account in this article, and the charge of 3DG/CNTs is deducted even though it is very little.

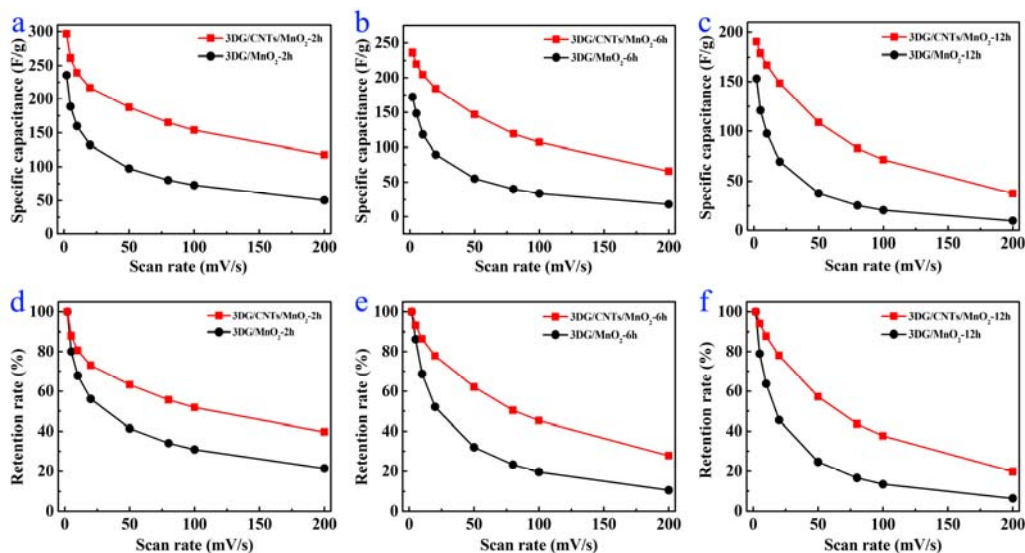


Fig. S5. Specific capacitance vs scan rate for 3DG/CNTs/MnO₂ and 3DG/MnO₂ electrodes with 2h (a), 6h (b) and 12h (c) MnO₂ loading; Specific capacitance retention of 3DG/CNTs/MnO₂ and 3DG/MnO₂ electrodes with 2h (d), 6h (e) and 12h (f) MnO₂ loading as the scan rate increasing from 2 mV/s.

The maximum specific capacitance of 2h, 6h and 12h MnO₂ loaded 3DG/CNTs/MnO₂ (3DG/MnO₂) were obtained as 296.8 (235.7), 236.2 (172.0) and 190.3 F/g (153.3 F/g) at scan rate of 2 mV/s, respectively. After the scan rate increased to 200 mV/s, the specific capacitance of 3DG/CNTs/MnO₂ (3DG/MnO₂) with 2h, 6h, and 12h MnO₂ loading reduced to 117.9 (50.5), 65.7 (18.1), and 37.5 F/g (9.8 F/g) and 39.7% (21.4%), 27.8% (10.5%), and 19.7% (6.4%) of the initial capacitance were remained, respectively.

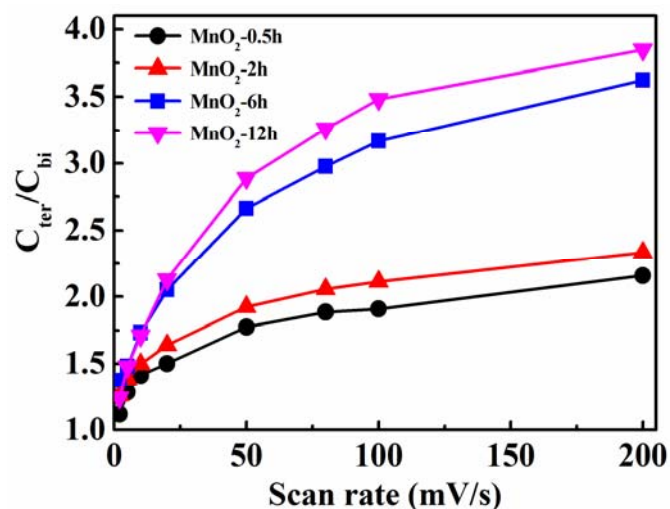


Fig. S6. Specific capacitance ratio vs scan rate of 3DG/CNTs/MnO₂ and 3DG/MnO₂ electrodes with different MnO₂ mass loading.

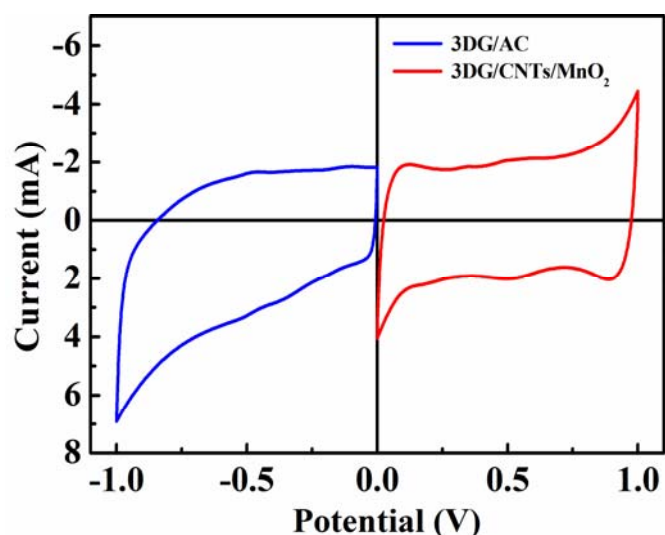


Fig. S7. Comparative CVs of 3DG/CNTs/MnO₂ and 3DG/AC electrodes at a scan rate of 10 mV/s.

The charge balance in the asymmetric supercapacitor was ensured by matching the mass of MnO₂ in positive (3DG/CNTs/MnO₂) and AC in negative (3DG/CNTs/MnO₂) electrodes. The CV of 3DG/CNTs/MnO₂ was measured within a potential range from 0 to 1 V, while that of 3DG/AC was measured within a potential range from -1 to 0 V at the same scan rate of 10 mV/s, as shown in Figure S6. Both CVs are relatively rectangular in shape and exhibit near mirror-image current response on voltage reversal, indicating an ideal capacitive behavior and approximately equal charge for both electrodes.¹ The specific capacitances calculated from the CVs are 239.3 F/g for 3DG/CNTs/MnO₂ electrode, and 217.6 F/g for 3DG/AC electrode. So, 3DG/AC with 0.92 mg AC have been matched according to the constant mass of MnO₂ (0.84 mg) in 3DG/CNTs/MnO₂.

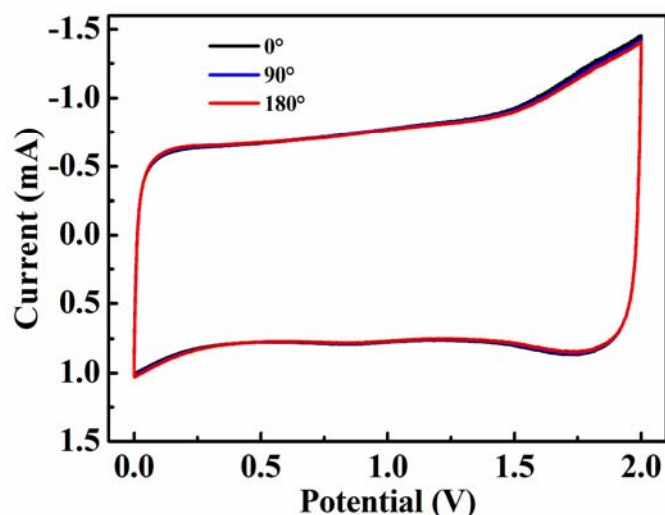


Fig. S8. From the CVs of the assembled asymmetric supercapacitor at different bending angles (scan rate: 10 mV/s), we can find that the electrochemical performance is almost not changed, demonstrating the potential application for flexible supercapacitor.

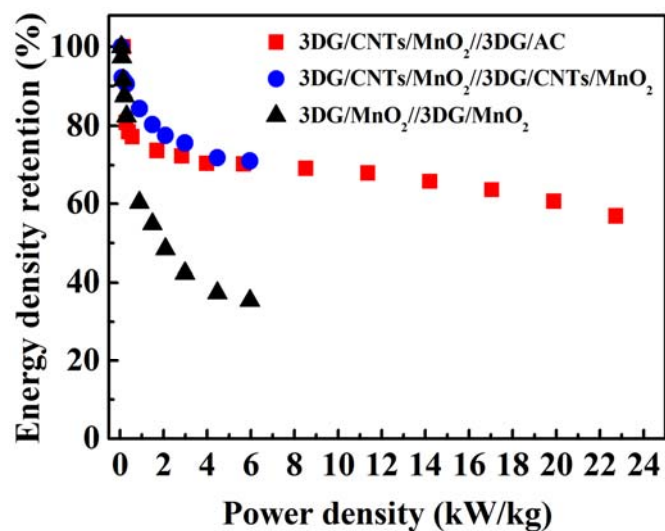


Fig. S9. Energy density retention of the three assembled supercapacitors.

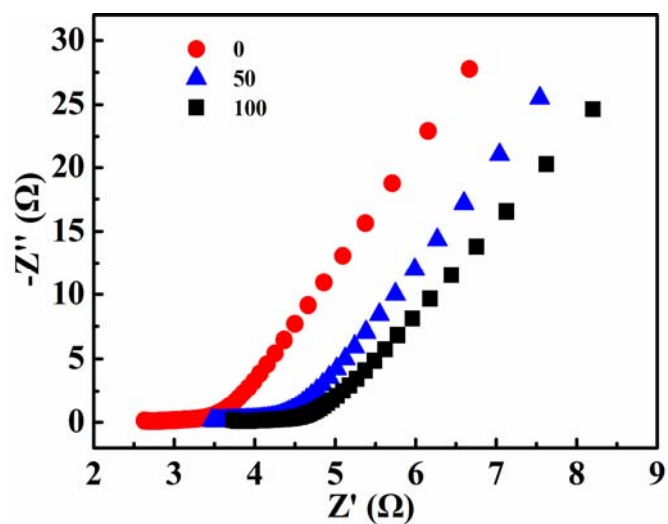


Fig. S10. Nyquist plots of the assembled asymmetric supercapacitor after different bending cycles (bending angle: 90°). It is indicated that the ESR show small increase after several bending cycles, but its capacitive performance (deduced from the slope in low frequency region) has changed weakly.

Table S1. Specific capacitance retention of the electrodes reported in literatures compared with our work.

Composite electrode	Scan rate range (mV/s)	Retention (%)	References
3DG/CNTs/MnO ₂	2 – 200	61.0	Our work
	2 – 800	43.8	
	2 – 1000	40.6	
	2 – 2000	31.5	
Graphene/MnO ₂ nanostructured textiles	2 – 100	~34.6	2
MnO ₂ /CNTs film	2 – 100	~28.8	3
Graphene/MnO ₂ /CNTs nanocomposites.	10 – 500	45	4
WO _{3-x} @Au@MnO ₂ core-shell NWs	10 – 100	~36.3	5
Au/MnO ₂ Core/Shell Nanowires	5 – 100	~44.1	6

Supplementary references

- 1 Z. Fan, J. Yan, T. Wei, L. Zhi, G. Ning, T. Li and F. Wei, *Adv. Funct. Mater.*, 2011, **21**, 2366.
- 2 G. Yu, L. Hu, M. Vosgueritchian, H. Wang, X. Xie, J. R. McDonough, X. Cui, Y. Cui and Z. Bao, *Nano Lett.*, 2011, **11**, 2905.
- 3 Y. Wang and I. Zhitomirsky, *Langmuir*, 2009, **25**, 9684.
- 4 Y. Cheng, S. Lu, H. Zhang, C. V. Varanasi and J. Liu, *Nano Lett.*, 2012, **12**, 4206.
- 5 X. Lu, T. Zhai, X. Zhang, Y. Shen, L. Yuan, B. Hu, L. Gong, J. Chen, Y. Gao, J. Zhou, Y. Tong and Z. L. Wang, *Adv. Mater.*, 2012, **24**, 938.
- 6 W. Yan, J. Y. Kim, W. Xing, K. C. Donovan, T. Ayvazian and R. M. Penner, *Chem. Mater.*, 2012, **24**, 2382.